LETTERS

Arctic hydrology during global warming at the Palaeocene/Eocene thermal maximum

Mark Pagani[1]*, Nikolai Pedentchouk[1]*, Matthew Huber[2]*, Appy Sluijs[3], Stefan Schouten[4], Henk Brinkhuis[3], Jaap S. Sinninghe Damsté[4,5], Gerald R. Dickens[6] & the Expedition 302 Scientists†

The Palaeocene/Eocene thermal maximum represents a period of rapid, extreme global warming ~55 million years ago, superimposed on an already warm world[1–3]. This warming is associated with a severe shoaling of the ocean calcite compensation depth[4] and a >2.5 per mil negative carbon isotope excursion in marine and soil carbonates[1–4]. Together these observations indicate a massive release of ^{13}C-depleted carbon[4] and greenhouse-gas-induced warming. Recently, sediments were recovered from the central Arctic Ocean[5], providing the first opportunity to evaluate the environmental response at the North Pole at this time. Here we present stable hydrogen and carbon isotope measurements of terrestrial-plant- and aquatic-derived *n*-alkanes that record changes in hydrology, including surface water salinity and precipitation, and the global carbon cycle. Hydrogen isotope records are interpreted as documenting decreased rainout during moisture transport from lower latitudes and increased moisture delivery to the Arctic at the onset of the Palaeocene/Eocene thermal maximum, consistent with predictions of poleward storm track migrations during global warming[6]. The terrestrial-plant carbon isotope excursion (about −4.5 to −6 per mil) is substantially larger than those of marine carbonates. Previously, this offset was explained by the physiological response of plants to increases in surface humidity[2]. But this mechanism is not an effective explanation in this wet Arctic setting, leading us to hypothesize that the true magnitude of the excursion—and associated carbon input—was greater than originally surmised. Greater carbon release and strong hydrological cycle feedbacks may help explain the maintenance of this unprecedented warmth.

PETM sediments, recovered from the Lomonosov ridge in the central Arctic Ocean during Integrated Ocean Drilling Program Expedition 302, are devoid of primary carbonates commonly used to assess palaeoclimate conditions. But they contain abundant organic components[5,7], including long-carbon-chain *n*-alkanes in the range *n*-C_{23} to *n*-C_{35}, with a strong odd-over-even carbon-chain character, and short-chain *n*-alkanes dominated by *n*-C_{17}. Long-chain *n*-alkanes with an odd-over-even predominance typically derive from the waxes of higher plants[8]. However, this common interpretation was questioned in a single study of modern Arctic organic carbon from the Laptev Sea, which inferred a marine source for these compounds[9]. Importantly, this interpretation does not apply to the Arctic during the Palaeogene, where the evidence used to support a marine origin for long-chain *n*-alkanes is lacking (Supplementary Information). Short-chain *n*-alkanes represent a mixture of aquatic sources, while *n*-alkane homologues dominated by *n*-C_{17} typify algal and photosynthetic bacterial input[10]. Even-chain-length *n*-alkanes in the range *n*-C_{14} to *n*-C_{22} are ascribed to bacteria[11]. Given lower abundances for even-chained *n*-alkanes during the PETM interval, we assume that *n*-C_{17} derives predominantly from algal sources, in accordance with other studies[12,13].

To assess changes in the hydrological system during the PETM, we measured the stable hydrogen isotope (δD) values of *n*-C_{29}, *n*-C_{27} and *n*-C_{17} (Fig. 1b). Although our understanding of compound-specific hydrogen isotope systematics is incomplete, it is clear that source water hydrogen is a primary signal recorded by *n*-alkyl lipids[14–16]. Our results implicate different water sources for high- and low-molecular-weight *n*-alkanes, with δD values of *n*-C_{17} recording the δD of Arctic surface waters, and δD values of *n*-C_{27} and *n*-C_{29} (*n*-$C_{27/29}$) reflecting the hydrogen isotopic composition of precipitation in the Arctic region.

Data from contemporary environments suggest an apparent hydrogen isotope fractionation of −130‰ to −100‰ for higher-plant-derived *n*-C_{29} and source water ($\Delta_{water\text{-}nC29}$)[13,15,17]. Smaller $\Delta_{water\text{-}nC29}$ values (that is, less negative than −100‰) have been reported for deciduous conifers grown under continuous light[18], similar to daylight conditions that characterize the Arctic growing season. A portion of this fractionation is potentially attributable to evapotranspiration, which acts to increase the δD value of leaf water used for lipid biosynthesis. However, rates of evapotranspiration are proportional to humidity[16], and given evidence for both high humidity (Supplementary Information) and fluvial runoff[7] during this interval of time, we assume that changes in the rates of evapotranspiration were negligible. Using $\Delta_{water\text{-}nC29}$ values of −130‰ and −100‰, we estimate that spring/summer precipitation had average δD values between −125‰ and −95‰ before the PETM, and −145‰ to −105‰ after the PETM, with much higher values (about −30‰ to −65‰) during the early phase of the event (Supplementary Information).

Our results suggest that Arctic PETM precipitation was substantially D-enriched relative to today, with hydrogen isotopic compositions comparable with modern, mid-latitude precipitation[19]. In general, the primary sources of atmospheric water vapour derive from the tropical and subtropical ocean. Poleward and altitudinal advection of air parcels approximately along isentropic surfaces[20] leads to cooling, condensation, an increase in the isotopic fractionation between the vapour and the condensate, and progressive isotopic distillation resulting in D-depleted high-latitude precipitation.

[1]Department of Geology and Geophysics, Yale University, PO Box 208109, New Haven, Connecticut 06520, USA. [2]Earth and Atmospheric Sciences Department and the Purdue Climate Change Research Center, Purdue University, 550 Stadium Mall Drive, West Lafayette, Indiana 47906, USA. [3]Palaeoecology, Institute of Environmental Biology, Utrecht University, Laboratory of Palaeobotany and Palynology, Budapestlaan 4, 3584 CD, Utrecht, The Netherlands. [4]Royal Netherlands Institute for Sea Research (NIOZ), Department of Marine Biogeochemistry and Toxicology, PO Box 59, 1790 AB, Den Burg, Texel, The Netherlands. [5]Faculty of Geosciences, Department of Earth Sciences, Utrecht University, Budapestlaan 4, 3584 CD, Utrecht, The Netherlands. [6]Department of Earth Sciences, Rice University, 6100 Main Street, Houston, Texas 77005, USA.
*These authors contributed equally to this work.
†A list of authors and affiliations appears at the end of the paper.

Deuterium-enriched Arctic precipitation during the PETM could have resulted from two end-member processes, including changes in proximal evaporative sources, or a decrease in large-scale (hemispheric to global) temperature gradients, such as the meridional temperature gradient as often assumed[21], or the vertical temperature gradient along isentropes characteristic of baroclinic eddy-induced mixing. Changes in evaporative sources during the PETM, large enough to explain the observed δD shift, would require a fundamental, global alteration in precipitation and evaporation. However, such effects are not supported by physical modelling or proxy data (Supplementary Information) and thus not considered likely.

Alternatively, decreased meridional and/or vertical temperature gradients would conspire to reduce rainout of subtropical water vapour by synoptic eddies[22], decrease isotopic distillation during vapour transport, and lead to D-enriched precipitation at high latitudes. If surface temperature gradients remained constant during the PETM[7], then changes in atmospheric static stability could have decreased rainout in the mid-latitudes. In either case, a decrease in temperature gradients should be expressed as a reduction in the meridional isotopic gradient. Support for this supposition comes from soil carbonate $\delta^{18}O$ records, which suggest that the δD value of mid-latitude PETM precipitation increased by only ~16‰ (refs 23, 24), compared to a δD increase of ~55‰ in the Arctic (Fig. 1b).

As a reduced meridional isotopic gradient implies less rainout along the source airmass's trajectory, more water vapour must have been transported to extreme high latitudes. Observations that support an increase in water supply to the Arctic during the PETM include the prevalence of low-salinity-tolerant organic-walled dinoflagellate cyst (dinocyst) assemblages, evidence for photic zone anoxia indicative of low-salinity surface waters (Fig. 1c), and strong seasonal runoff[7]. This scenario suggests that the latitude of maximum latent heat flux divergence (today at ~40°) could have been situated much closer to the poles, broadly consistent with climate model results[6,22].

Enhanced moisture and latent heat transport from the subtropics to the Arctic region could have resulted from the nonlinear dependence of the saturation specific humidity of subtropical air parcels as a function of temperature[1,6], and/or a reduction of mid-latitude precipitation. Thus, as a corollary to our argument for an increase in poleward water vapour transport, we suggest that the subtropics and parts of the mid-latitudes experienced less net precipitation during the PETM.

Changes in surface water salinity were evaluated from δD_{nC17}. Limited analysis of lake sediments and aquatic plants suggest that values of $\Delta_{water\text{-}nC17}$ range from about −160‰ to −80‰ (refs 13, 15, 17). In order to determine plausible values of $\Delta_{water\text{-}nC17}$ for these Arctic sediments, we modelled the relationship between the δD of Arctic surface water, and the isotopic compositions of precipitation (that is, runoff) that acts to freshen the Arctic and alter its salinity (Fig. 2a). Our results suggest that δD values of Arctic surface waters were approximately −41‰ to −52‰, resulting in a $\Delta_{water\text{-}nC17}$ of −70‰ to −80‰.

The δD_{nC17} record, in conjunction with a $\Delta_{water\text{-}nC17}$ of −75‰, indicate that the surface water salinity of the Arctic Ocean decreased as the PETM progressed, followed by a rapid increase in salinity towards the end of the climate anomaly (Fig. 2b). Low-salinity surface waters correspond with the presence of low-salinity-tolerant dinocyst assemblages and the occurrence of isorenieratene derivatives[7] (Fig. 1c), biomarkers indicative of anoxia within the photic zone. This confluence suggests that water column stratification was promoted, in large part, by low-salinity surface water[7], given that seawater density variations are determined primarily by salinity variations in the temperature range indicated by TEX_{86} temperature estimates (Fig. 1c). Termination of these conditions and a progressive

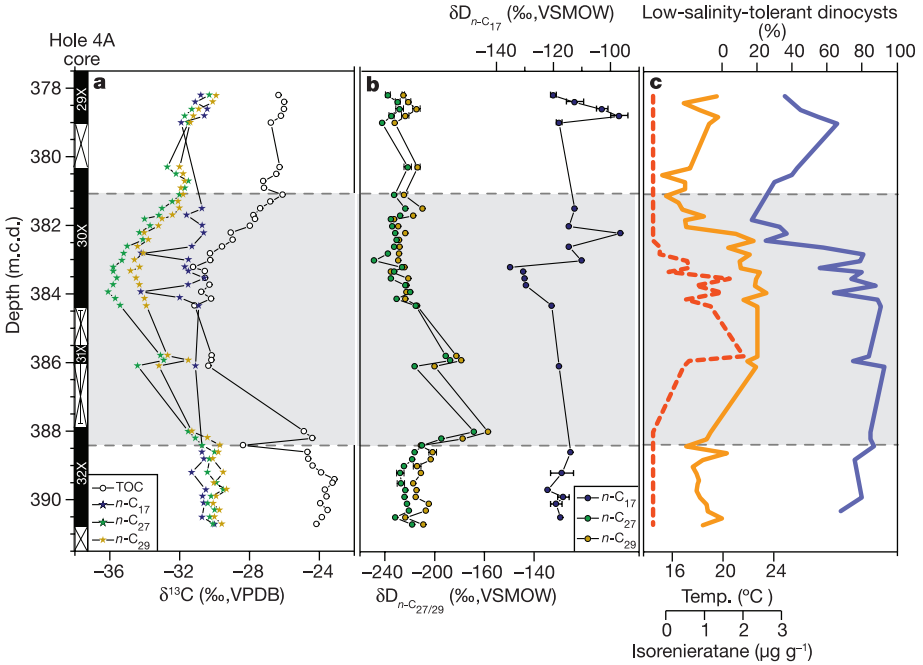

Figure 1 | Stable isotope results, and data on sea surface temperature, dinocysts and biomarkers. **a**, Stable carbon isotope data. m.c.d., metres composite depth below sea floor; TOC, total organic carbon. **b**, Stable hydrogen isotope data. Error bars represent the range of values based on duplicate measurements. **c**, Data from ref. 7. Orange line, sea surface temperatures based on the TEX'_{86} index. Blue line, relative abundances of dinocysts produced by dinoflagellate species that were tolerant of low salinity. Red dashed line, absolute abundances of isorenieratene derivatives, biomarkers derived from photosynthetic green sulphur bacteria. The presence of these bacteria implies water column stratification and the development of photic zone euxinia. The leftmost (recovery) column shows core numbers: black bars, recovered material; white bars, missing material. Error bars connected to Core 31X indicate the uncertainty of its stratigraphic position (see ref. 7). Grey-shaded area indicates the PETM.

change to fewer low-salinity-tolerant dinocyst assemblages[7] coincide with a trend towards more saline surface waters by the end of the climate anomaly (Fig. 2b).

Further insight into the nature of Arctic climate change is provided by the carbon isotopic ($\delta^{13}C$) compositions of the same *n*-alkyl lipids. The $\delta^{13}C$ values of *n*-$C_{29/27}$ show a large negative carbon isotope excursion (CIE) across the PETM that tracks the $\delta^{13}C$ record of total organic carbon[7] ($\delta^{13}C_{TOC}$) (Fig. 1a), but are ~6‰ more negative than $\delta^{13}C_{TOC}$ values before and after the CIE, and ~3‰ to 5‰ more negative during the CIE. This correlation, both in trend and isotopic offset, suggests that the TOC is substantially influenced by terrestrial components.

Importantly, the CIE from higher plant *n*-alkanes (approximately −4.5‰ to −6‰) is substantially larger than the CIE anomaly (about −2.5‰ to −3‰) generally recorded in bulk marine carbonate and benthic foraminifera[1,3], but similar to those recorded in soil carbonates from mid-latitudes[2] and some planktonic foraminiferal records[3]. To explain the larger terrestrial CIE elsewhere, it has been suggested that soil moisture and humidity increased during the PETM, amplifying the carbon isotopic fractionation associated with terrestrial photosynthesis (CIF)[2]. In this model, a larger CIF due to increasing humidity and soil moisture has to overcome the antagonistic effect of decreasing CIF due to higher temperatures during the PETM[2,7]. In order for this model to explain our data, latest Palaeocene soil moistures and humidity levels surrounding the Arctic Ocean would have to have been quite low, with soil moistures at or below 40% (ref. 2), similar to those found in modern arid-to-semiarid environments (Supplementary Information). A dry Arctic is difficult to justify, given palaeoecological reconstructions from high-latitude coal distributions and terrestrial palaeobotanical records that strongly support the prevalence of mesic to wet climate conditions throughout the Arctic region during the Palaeocene and Eocene (Supplementary Information). Conditions associated with analogous modern tropical and warm temperature forests can be used to predict that the Palaeogene Arctic maintained an average relative humidity of >70%, with soil moistures >60% (Supplementary Information)—estimates that agree well with fully coupled climate model simulations (Supplementary Information). The accumulative evidence, including the δD results from this study, and evidence for high seasonal discharge and low-salinity surface waters during the PETM[7], point to a warm and moist late Palaeocene–early Eocene Arctic region, with increased precipitation expressing itself largely as increased runoff[7].

Other possibilities exist to explain this CIE discrepancy between higher plant *n*-alkanes and marine carbonate records. For example, given potentially more negative $\delta^{13}C$ values for angiosperms relative to gymnosperms[25], an increase in angiosperms relative to gymnosperms during the PETM[7] could possibly explain a larger isotopic excursion in $\delta^{13}C_{TOC}$ relative to marine carbonates. However, modern isotopic offsets between gymnosperms and angiosperms probably result from differences in water use efficiency[25] under low CO_2 concentrations. Therefore, more humid environmental conditions during the PETM in the Arctic would have arguably minimized isotopic distinctions between these two plant types. In addition, the $\delta^{13}C$ difference between *n*-alkanes and bulk leaf carbon is potentially smaller for angiosperms relative to gymnosperms[17]. Thus, the $\delta^{13}C$ excursion in *n*-$C_{29/27}$ potentially represents a minimum change—if flora shifts occurred in the Arctic region during the PETM, and whole plant $\delta^{13}C$ values of gymnosperms and angiosperms were similar. Finally, similar ecosystem shifts would need to have synchronously occurred globally to account for terrestrial ^{13}C excursions of the same magnitude elsewhere.

Rather than systematically explaining a similar observation by different processes, it is possible that the CIE expressed by higher plant *n*-alkanes reflects the true $\delta^{13}C$ change of atmospheric carbon dioxide in equilibrium with the ocean during the PETM. Such a scenario implies that foraminiferal $\delta^{13}C$ values do not accurately represent the full CIE of dissolved inorganic carbon in the ocean owing to effects related to dissolution[4] and changes in pH (ref. 26). We note that in marine cores with limited carbonate dissolution, the observed $\delta^{13}C$ excursion recorded from shallow-dwelling plankton is about −4‰ (ref. 3), which is close to our value. Further consideration of the carbon isotope effect related to changes in pH allow for the ^{13}C-enrichment of carbonates in the range of 0.5‰ (refs 1, 2). Therefore, it is possible to account for rather similar terrestrial and marine CIEs. Importantly, evidence for a CIE of about −4.5‰ to −5‰ nearly doubles the mass estimate for the release of carbon during this time, and more closely approximates the carbon concentration required to account for the observed shoaling of the ocean carbonate compensation depth[4], as well as changes in global temperatures.

The $\delta^{13}C$ values of *n*-C_{17} are nominally −30‰, similar to those of *n*-$C_{29/27}$ before and following the PETM, but are ^{13}C-enriched relative to higher plant *n*-alkanes during the PETM (Fig. 1a). In modern settings, algal organic carbon is consistently ^{13}C-enriched relative to terrestrial C_3 plants. Similar $\delta^{13}C$ values for algal and higher plant organic carbon before and after the PETM is consistent with a high atmospheric CO_2 environment[27,28]. However, the relative increase in the $\delta^{13}C$ of *n*-C_{17} during the PETM must have resulted from physiological factors that overwhelmed the influence of ^{13}C-depleted carbon, such as increases in the volume to surface area of cells, and/or algal growth rates[29], consistent with evidence for eutrophy and nutrient-rich conditions during the PETM[7]. Interestingly, changes in primary productivity appear to have occurred in other ocean regions[30] and are thought to have played a critical role in the carbon cycle response to environmental change. Given the relative isolation of the Arctic from other ocean basins during this time[7], widespread changes in primary production were probably linked to changes in riverine nutrient supply; this implicates the hydrological cycle as an important agent forcing biological and environmental change during the PETM.

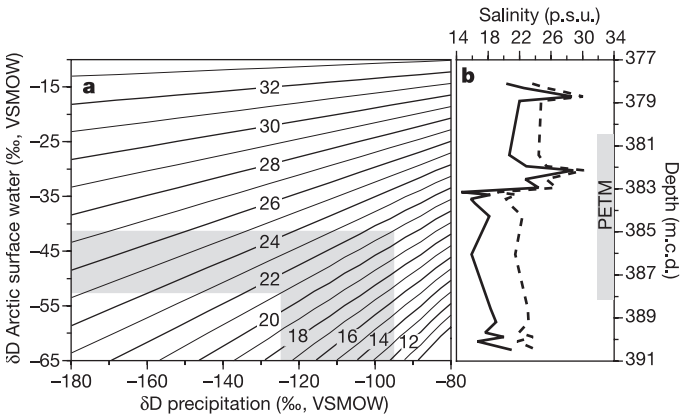

Figure 2 | δD of precipitation and Arctic surface water, and salinity. **a**, Calculations[31] of Arctic Ocean salinity (numbers on contours, in practical salinity units, p.s.u.) assume an ice-free, global seawater δD value of −8‰ (VSMOW) and a global salinity of 34 p.s.u. Shaded bands represent pre-PETM conditions, given a salinity of 21 p.s.u. (Supplementary Information) and δD values of precipitation from δD_{nC29}, yielding a δD estimate for Arctic surface water (δD_{AW}) of about −41‰ to −52‰, resulting in a $\Delta_{water\text{-}nC17}$ value (see text) of about −70‰ to −80‰. **b**, Surface water salinity calculations, derived from δD_{AW}; δD_{AW} was calculated from δD_{nC17}, assuming a $\Delta_{water\text{-}nC17}$ value of −75‰, and the δD of precipitation derived from δD_{nC29} assuming $\Delta_{water\text{-}nC29}$ values of −100‰ (solid line) and −130‰ (dashed line).

METHODS

Sample extraction. Sediments were extracted with dichloromethane using an accelerated solvent extraction system (ASE 300; Dionex Corporation) at 125 °C,

1,500 p.s.i., for 25 min. Lipid fractions were separated by column chromatography (70–230 mesh) using an elution sequence of hexane, hexane/dichloromethane (9:1 v/v) and dichloromethane/methanol (2:1 v/v). Cyclic and branched alkanes were separated from normal and isoalkanes by adduction with urea. The hydrocarbon fraction was dried under a stream of N_2 and dissolved in a mixture of methanol-saturated urea, pentane and acetone (200 μl each). The resulting urea crystals were extracted with hexane, yielding cyclic/branched alkanes. Remaining urea crystals were dissolved in 500 μl of H_2O and 500 μl of methanol, then extracted with hexane to yield the *n*-alkane fraction.

Analysis. The adducted fraction was analysed for stable carbon and hydrogen isotopic compositions on a Thermo Finnigan MAT 253 mass spectrometer interfaced with a Thermo Finnigan Trace GC Combustion III (for carbon measurements) and High Temperature Conversion (for hydrogen measurements) systems. Individual *n*-alkanes were separated using a J&W Scientific DB-1 capillary column (60 m × 0.25 mm × 0.25 μm). The gas chromatograph oven was programmed from 60 °C (held for 1 min) at 6 °C min^{-1} to 320 °C and held for 25 min isothermally. A programmed temperature vaporizing injector was used. Helium was used as a carrier gas with a column flow rate of 2.0 ml min^{-1}. Carbon isotopic compositions are expressed relative to the VPDB standard, based on an in-house reference gas calibrated against the OzTech standard ($\delta^{13}C = -40.61‰$). The analytical accuracy and precision of the MAT 253 mass spectrometer during carbon isotope measurements were ±0.2‰ (the root-mean-square error), based on an *n*-C_{20} alkane standard injected daily. The standard error of *n*-alkane $\delta^{13}C$ measurements (based on duplicates of 22 samples) was ±0.8‰ or better (Supplementary Information).

Pyrolytic conversion of organic hydrogen to H_2 was conducted at 1,400 °C. Measurements of the H_3^+ factor (the proportionality constant between the concentration of H_2 and H_3^+ in the mass spectrometer) were determined daily using H_2 reference gas. The H_3^+ factor varied between 15.27 and 16.11 p.p.m. nA^{-1} over a period of 23 days, averaging 15.70 p.p.m. nA^{-1}, with a standard deviation of 0.24 p.p.m. nA^{-1}. H_2 peak heights varied over an eightfold range, which was in the range of most of the H_2 peaks from analysed compounds.

Errors. The precision of isotopic measurements of H_2 reference gas after H_3^+ correction was ±0.9‰ or better. The analytical accuracy and precision of the system were determined using an externally co-injected standard mixture of *n*-C_{16} to *n*-C_{30} alkanes and 5α-androstane (isotopic ratios were measured off-line by A. Schimmelmann, Biogeochemical Laboratories, Indiana University), which were analysed at least once per day. The root-mean-square error for hydrogen isotopic measurements of these compounds was 3.4‰ ($n = 240$). Hydrogen isotopic compositions of *n*-alkanes are reported based on duplicate analyses. δD values are expressed relative to the VSMOW standard, based on an in-house reference gas adjusted daily using a 5α-androstane standard. The standard error of *n*-C_{17}, *n*-C_{27} and *n*-C_{29} δD measurements was generally less than ±5‰, reaching ±6‰ only in a few cases (see Supplementary Information).

Received 6 July 2005; accepted 3 July 2006.

1. Zachos, J. *et al.* A transient rise in tropical sea surface temperature during the Paleocene-Eocene thermal maximum. *Science* **302,** 1551–1554 (2003).
2. Bowen, G. J., Beerling, D. J., Koch, P. L., Zachos, J. C. & Quattlebaum, T. A humid climate state during the Palaeocene/Eocene thermal maximum. *Nature* **432,** 495–499 (2004).
3. Thomas, D. J., Zachos, J. C., Bralower, T. J., Thomas, E. & Bohaty, S. Warming the fuel for the fire: evidence for the thermal dissociation of methane hydrate during the Paleocene-Eocene thermal maximum. *Geology* **30,** 1067–1070 (2002).
4. Zachos, J. C. *et al.* Rapid acidification of the ocean during the Paleocene-Eocene thermal maximum. *Science* **308,** 1611–1615 (2005).
5. Backman, J., Moran, K., McInroy, D. B., Mayer, L. A. & Expedition Scientists. Arctic Coring Expedition (ACEX). *Proc. IODP* **302** l/doi:10.2204/iodp.proc.302.2006 (Integrated Ocean Drilling Program Management International, College Station, Texas, 2006).
6. Caballero, R. & Langen, P. The dynamic range of poleward energy transport in an atmospheric general circulation model. *Geophys. Res. Lett.* **32**, doi:10.1029/2004GL021581 (2005).
7. Sluijs, A. *et al.* Subtropical Arctic Ocean temperatures during the Palaeocene/Eocene thermal maximum. *Nature* **441,** 610–613 (2006).
8. Eglinton, G. & Hamilton, R. J. Leaf epicuticular waxes. *Science* **156,** 1322–1335 (1967).
9. Zegouagh, Y., Derenne, S., Largeau, C., Bardoux, G. & Mariotti, A. Organic matter sources and early diagenetic alteration in Arctic surface sediments (Lena River delta and Laptev Sea, Eastern Siberia), II. Molecular and isotopic studies of hydrocarbons. *Org. Geochem.* **28,** 571–583 (1998).
10. Han, J. & Calvin, M. Hydrocarbon distribution of algae and bacteria, and microbiological activity in sediments. *Proc. Natl Acad. Sci. USA* **64,** 436–443 (1969).
11. Grimalt, J. & Albaiges, J. Sources and occurrence of C_{12-22} *n*-alkane distributions with even carbon-number preference in sedimentary environments. *Geochim. Cosmochim. Acta* **51,** 1379–1384 (1987).
12. Muri, G., Wakeham, S. G., Pease, T. K. & Faganeli, J. Evaluation of lipid biomarkers as indicators of changes in organic matter delivery to sediments from Lake Planina, a remote mountain lake in NW Slovenia. *Org. Geochem.* **35,** 1083–1093 (2004).
13. Sachse, D., Radke, J. & Gleixner, G. Hydrogen isotope ratios of recent lacustrine sedimentary n-alkanes record modern climate variability. *Geochim. Cosmochim. Acta* **68,** 4877–4889 (2004).
14. Sternberg, L. D. L. D/H ratios of environmental water recorded by D/H ratios of plant lipids. *Nature* **333,** 59–61 (1988).
15. Sauer, P. E., Eglinton, T. I., Hayes, J. M., Schimmelmann, A. & Sessions, A. L. Compound-specific D/H ratios of lipid biomarkers from sediments as a proxy for environmental and climatic conditions. *Geochim. Cosmochim. Acta* **65,** 213–222 (2001).
16. Yakir, D. in *Stable Isotopes* (ed. Griffiths, H.) 147–168 (BIOS Scientific Publishers, Oxford, 1998).
17. Chikaraishi, Y. & Naraoka, H. Compound-specific δD and $\delta^{13}C$ analyses of n-alkanes extracted from terrestrial and aquatic plants. *Phytochemistry* **63,** 361–371 (2003).
18. Yang, H., Equiza, A. M., Jagels, R., Pagani, M. & Briggs, D. Carbon and hydrogen isotopic compositions of deciduous conifers under a continuous-light environment: implications for the interpretation of the high-latitudinal plant isotope record at the PETM. (Salt Lake City Annual Meeting, October 16–19, The Geological Society of America, 2005).
19. Bowen, G. J. & Revenaugh, J. Interpolating the isotopic composition of modern meteoric precipitation. *Wat. Resour. Res.* **39**, doi:10.1029/2003WR002086 (2003).
20. Pierrehumbert, R. T. Lateral mixing as a source of subtropical water vapor. *Geophys. Res. Lett.* **25,** 151–154 (1998).
21. Boyle, E. A. Cool tropical temperatures shift the global $\delta^{18}O$-T relationship: An explanation for the ice core $\delta^{18}O$-borehole thermometry conflict? *Geophys. Res. Lett.* **24,** 273–276 (1997).
22. Pierrehumbert, R. T. The hydrologic cycle in deep time climate problems. *Nature* **419,** 191–198 (2002).
23. Koch, P. L. *et al.* in *Causes and Consequences of Globally Warm Climates in the Early Paleogene* (eds Wing, S. L., Gingerich, P. D., Schmitz, B. & Thomas, E.) 49–64 (Special Paper 369, Geological Society of America, Boulder, 2003).
24. Fricke, H. C., Clyde, W. C., O'Neil, J. R. & Gingerich, P. D. Evidence for rapid climate change in North America during the latest Paleocene thermal maximum: oxygen isotope compositions of biogenic phosphate from the Bighorn Basin (Wyoming). *Earth Planet. Sci. Lett.* **160,** 193–208 (1998).
25. Leavitt, S. W. & Newberry, T. Systematics of stable-carbon isotopic differences between gymnosperm and angiosperm trees. *Plant Physiol.* **11,** 257–262 (1992).
26. Spero, H. J., Bijma, J., Lea, D. W. & Bernis, B. E. Effect of seawater carbonate concentration on foraminiferal carbon and oxygen isotopes. *Nature* **390,** 497–500 (1997).
27. Arthur, M. A., Walter, D. E. & Claypool, G. E. Anomalous ^{13}C enrichment in modern marine organic carbon. *Nature* **315,** 216–218 (1985).
28. Pagani, M., Zachos, J. C., Freeman, K. H., Tipple, B. & Bohaty, S. Marked decline in atmospheric carbon dioxide concentrations during the Paleogene. *Science* **309,** 600–603 (2005).
29. Popp, B. *et al.* Effect of phytoplankton cell geometry on carbon isotopic fractionation. *Geochim. Cosmochim. Acta* **62,** 69–77 (1998).
30. Bujak, J. P. & Brinkhuis, H. in *Late Paleocene - Early Eocene Biotic and Climatic Events in the Marine and Terrestrial Records* (eds Aubry, M.-P., Lucas, S. G. & Berggren, W. A.) 277–295 (Columbia Univ. Press, New York, 1998).
31. Railsback, L. B., Anderson, T. F., Ackerly, S. C. & Cisne, J. L. Paleoceanographic modeling of temperature-salinity profiles from stable isotopic data. *Paleoceanography* **4,** 585–591 (1989).

Supplementary Information is linked to the online version of the paper at www.nature.com/nature.

Acknowledgements M.P. thanks K. Turekian for conversations, and G. Bowen for comments and suggestions that substantially improved the manuscript. M.H. thanks the Purdue Research Foundation, ITaP, NCAR, NSF and L. C. Sloan for support for this research. A.S. thanks Utrecht Biogeology Centre for funding. H.B. thanks NWO, the Netherlands Organization for Scientific Research, and Utrecht University for enabling participation. We appreciate technical assistance provided by C. Valache, A. McLawhorn and G. Olack. This research used samples and data provided by the Integrated Ocean Drilling Program (IODP), which is sponsored by the US NSF and participating countries under the management of Joint Oceanographic Institutions (JOI) Inc.

Author Information Reprints and permissions information is available at npg.nature.com/reprintsandpermissions. The authors declare no competing financial interests. Correspondence and requests for materials should be addressed to M.P. (mark.pagani@yale.edu).

Expedition 302 Scientists (those not listed above): Jan Backman[1], Steve Clemens[2], Thomas Cronin[3], Frédérique Eynaud[4], Jérôme Gattacceca[5], Martin Jakobsson[6], Ric Jordan[7], Michael Kaminski[8], John King[9], Nalân Koc[10], Nahysa C. Martinez[11], David McInroy[12], Theodore C. Moore Jr[13], Matthew O'Regan[9], Jonaotaro Onodera[14], Heiko Pälike[15], Brice Rea[16], Domenico Rio[17], Tatsuhiko Sakamoto[18], David C. Smith[9], Kristen E. K. St John[19], Itsuki Suto[20], Noritoshi Suzuki[21], Kozo Takahashi[14], Mahito Watanabe[22] & Masanobu Yamamoto[23]

[1]Department of Geology and Geochemistry, Stockholm University, Stockholm, SE-10691, Sweden. [2]Geological Sciences, Brown University, 324 Brook Street, PO Box 1846, Providence, Rhode Island 02912-1846, USA. [3]US Geological Survey, Eastern Earth Surface Processes Team, 926A USGS National Center, Reston, Virginia 20192, USA. [4]Department de Géologie et Océanographie, Université Bordeaux 1, Avenue des facultés, c/o Bernei Housen, 33405 Talence Cedex, France. [5]Department of Geophysics, CEREGE (CNRS)/University of Aix-Marseille 3, BP80, 13545 Aix-en-Provence Cedex 4, France. [6]Department of Geology and Geochemistry, Stockholm University, 10691 Stockholm, Sweden. [7]Department of Earth and Environmental Sciences, Faculty of Science, Yamagata University, 1-4-12 Kojirakawa-machi, Yamagata 990-8560, Japan. [8]Department of Earth Sciences, University College London, Gower Street, London WC1E 6BT, UK. [9]Graduate School of Oceanography, University of Rhode Island, Narragansett Bay Campus, South Ferry Road, Narragansett, Rhode Island 02882, USA. [10]Norwegian Polar Institute, Polar Environmental Center, N-9296 Tromsø, Norway. [11]Department of Earth Sciences, Boston University, 685 Commonwealth Avenue, Boston, Massachusetts 02215, USA. [12]British Geological Survey, Murchison House, West Mains Road, Edinburgh EH9 3LA, UK. [13]Geological Sciences, University of Michigan, Ann Arbor, Michigan 48109-1063, USA. [14]Department of Earth and Planetary Sciences, Graduate School of Sciences, Kyushu University, Hakozaki 6-10-1, Higashi-ku, Fukuoka 812-8581, Japan. [15]School of Ocean and Earth Science, University of Southampton, Southampton Oceanography Centre, European Way, Southampton SO14 3ZH, UK. [16]Department of Geography and Environment, School of Geosciences, University of Aberdeen, Elphinstone Road, Aberdeen AB24 3UF, UK. [17]Department of Geology, Paleontology and Geophysics, University of Padova, Via Giotto 1 I-35137 Padova, Italy. [18]Institute for Research on Earth Evolution (IFREE), Japan Agency for Marine-Earth Science and Technology (JAMSTEC), Natsushima-cho 2-15, Yokosuka 237-0061, Japan. [19]Department of Geology and Environmental Science, MSC7703, James Madison University, Harrisonburg, Virginia 22807, USA. [20]Institute of Life and Environmental Science, University of Tsukuba, Tennoudai 1-1-1, Tsukuba, Ibaraki 305-8572, Japan. [21]Institute of Geology and Paleontology, Graduate School of Science, Tohoku University, Aramaki, Aoba, Aoba-ku, Sendai City 980-8578, Japan. [22]Institute of Geoscience, National Institute of Advanced Industrial Science, and Technology (Geological Survey of Japan), AIST Tsukuba Central 7, Higashi-1-1-1, Tsukuba, Ibaraki 305-8567, Japan. [23]Graduate School of Environmental Earth Science, Hokkaido University, Kita-10, Nishi-5, Kita-ku, Sapporo 060-0810, Japan.